Electronic-structure study of $Ni_{81}Cr_{15}B_4$ metallic glass using photoemission spectroscopy

S. K. Kulkarni, M. G. Thube, and Arun S. Nigavekar
Department of Physics, University of Poona, Pune 411 007, Maharashtra, India
(Received 24 February 1987)

X-ray- and ultraviolet-photoelectron spectroscopic studies of the core levels and the valence band of amorphous and crystalline (annealed at 800 K) $Ni_{81}Cr_{15}B_4$ metallic glass are presented, and a comparison has been made of the valence-band spectra with those of the constituent elements. The single broad band appearing in the vicinity of the Fermi level in the spectrum of amorphous $Ni_{81}Cr_{15}B_4$ is attributed to the *d*-band combination of both nickel and chromium. The low-lying states arise due to hybridization of metal-metalloid levels. The Ni_3B phase has been detected in crystalline $Ni_{81}Cr_{15}B_4$. The binding energy changes in the Ni $2p_{3/2}$, Cr $2p_{3/2}$, and B 1*s* levels, the variation of the Ni $2p_{3/2}$ satellite intensity, and asymmetry-index changes for the core lines have been used to support the above picture as well as to arrive at a comprehensive understanding of the density-of-states variation at the Fermi level. The charge-transfer mechanism between constituent elements in metallic glasses is also discussed.

I. INTRODUCTION

Metallic glasses, materials prepared by rapid quenching of melts, are characterized by their absence of long-range atomic order. Since the disordered state is thermodynamically unstable, stability of metallic glasses against crystallization has become a focus of many investigations.[1-5] A number of criteria are available[6,7] which predict the formation of a glassy state in alloys. Some of these include large atomic size differences, valence differences among the constituents, near eutectic composition, and negative heats of mixing. Attempts have also been made to establish a correlation between glassy state formation and variation of density of states (DOS) in the valence band.[1,8] The nearly-free-electron approach of Nagel and Tauc[8] for amorphous materials predicts a reduction in the density of states in the vicinity of the Fermi level (E_F). Experimental evidence for this has been given by Haüssler *et al.*[9] for Au_xSn_{100-x} ($0 \lesssim x \lesssim 100$) films in amorphous as well as in the crystalline state. Even then it is yet doubtful whether this may be applicable to metallic glasses containing large amounts of transition elements that have large DOS (at least for one of the constituents) near Fermi level. Thus there remains a large number of metallic glasses like transition-metal–transition-metal glasses (*T-T*), transition-metal–normal-metal (*T-N*), or transition-metal–metalloid (*T-M*) for which the validity of the Nagel and Tauc model is uncertain. Since the metallic glasses are characterized by a high coordination number, assuming an fcc-like structure for metallic glasses, Moruzzi *et al.*[1,10] showed that transition-metal–transition-metal glassy alloys tend to have a large density of states near the Fermi level (E_F). Large density of states in the vicinity of the Fermi level is a characteristic of an unstable structure. It was therefore proposed by Moruzzi *et al.*[10] that in transition-metal–transition-metal glasses (*T-T*), the chemical, as well as the structural, orders are not stable, which is evident from the high density of states in the vicinity of the Fermi level. Further it was suggested that since the metallic glasses are formed in the composition range near the deep eutectic in the phase diagram, glassy solids are not significantly more stable than the liquid and the metallic glasses do not possess short-range stability. On an atomic scale, therefore, regions of different stoichiometry with disordered structure are expected. However, it appears that more experiments are necessary in order to understand the interrelationship between the stoichiometry, the stability, and the electronic structure of metallic glasses. Our recent measurements of density of states in the valence-band region for the Ni-P system, using x-ray-photoelectron spectroscopy, have revealed[11] a reduction in DOS for a composition near deep eutectic and an increase in the DOS for composition away from the eutectic with reference to DOS for Ni in the vicinity of the Fermi level. There is therefore a need to investigate electronic structure in a variety of transition-metal–metalloid systems.

Here, we report the photoelectron spectroscopic investigations on a $Ni_{81}Cr_{15}B_4$ metallic glass sample as well as its crystallized form. Nickel exhibits a large *d*-band maximum[12] in the vicinity and chromium slightly away[13] from the Fermi level, whereas in boron the 2*p* states lie at 5 eV below the Fermi level.[14] It is, therefore, interesting to see how the DOS for *a*-$Ni_{81}Cr_{15}B_4$ is related to those of nickel 3*d*, chromium 3*d* and boron 2*p* bands. Measurements have been carried out on the *c*-$Ni_{81}Cr_{15}B_4$ sample also and are compared with those of the amorphous sample in order to find out the correlation, if any, between the DOS in the valence band and the structure (amorphous or crystalline) or the material. Besides the valence-band structure obtained by using the x-ray-photoelectron spectroscopy (XPS) and the ultraviolet-photoelectron spectroscopy (UPS), use has been made of observed satellite structure as well as an asymmetry index in core level spectra to qualitatively determine the trends in the variation of DOS in the region near the Fermi level.

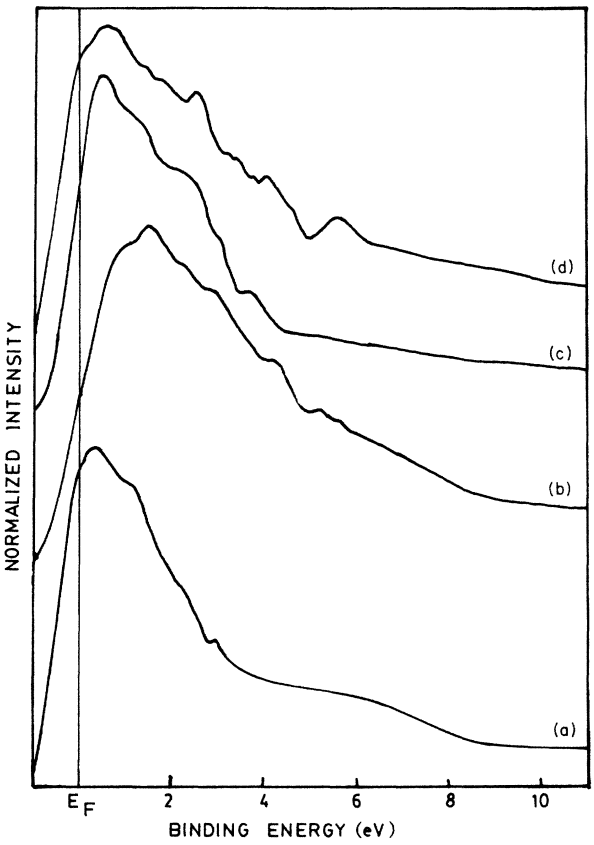

FIG. 1. Valence bands of (a) polycrystalline nickel, (b) polycrystalline chromium, (c) a-$Ni_{81}Cr_{15}B_4$ and (d) c-$Ni_{81}Cr_{15}B_4$ obtained using Mg $K\alpha$ ($h\nu = 1253.6$ eV) source.

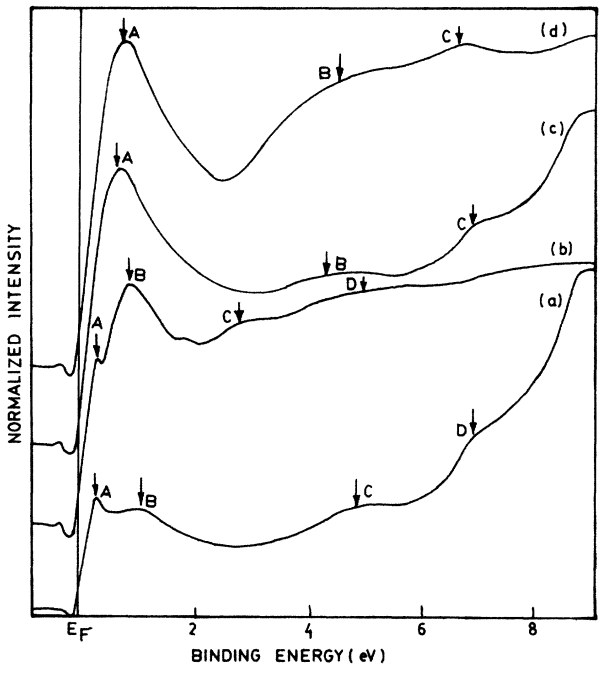

FIG. 2. Valence bands of (a) polycrystalline nickel, (b) polycrystalline chromium, (c) a-$Ni_{81}Cr_{15}B_4$, and (d) c-$Ni_{81}Cr_{15}B_4$ obtained using He I ($h\nu = 21.2$ eV) source.

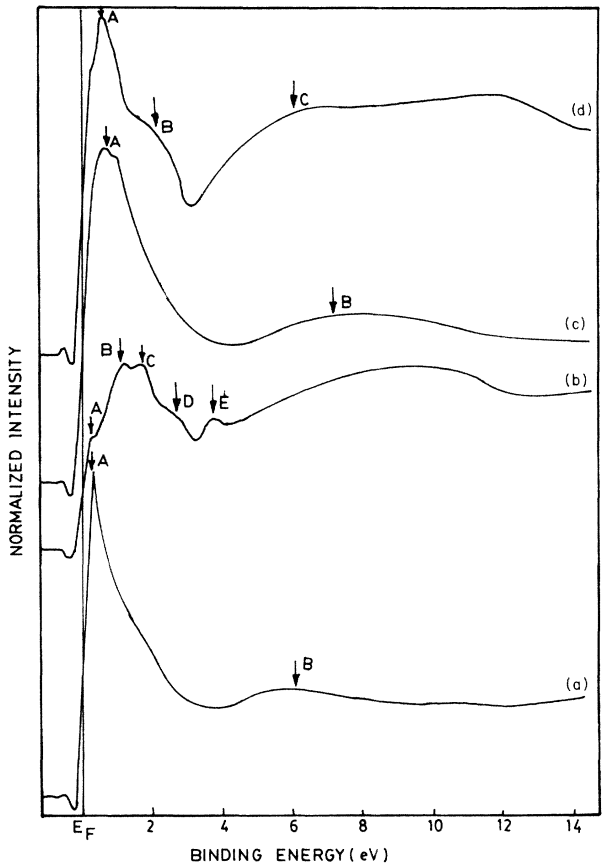

FIG. 3. Valence bands of (a) polycrystalline nickel, (b) polycrystalline chromium, (c) a-$Ni_{81}Cr_{15}B_4$, and (d) c-$Ni_{81}Cr_{15}B_4$ obtained using He II ($h\nu = 40.8$ eV) source.

II. EXPERIMENT

The $Ni_{81}Cr_{15}B_4$ metallic glass sample under investigation was received from Vakuumschemelze, West Germany. It was in the form of a thin ribbon ~ 50 μm thick and 2 cm wide. The amorphous nature of the sample was checked by x-ray diffraction (XRD) analysis carried out

TABLE I. Core level binding energies of various levels determined using a Mg $K\alpha$ ($h\nu = 1253.6$ eV) source in a-$Ni_{81}Cr_{15}B_4$, c-$Ni_{81}Cr_{15}B_4$, and of constituting elements in their elemental form.

	Binding energy in eV		
Core level	a-$Ni_{81}Cr_{15}B_4$	c-$Ni_{81}Cr_{15}B_4$	Pure elements
Ni $2p_{3/2}$	853.0	853.0	852.8
Ni $3s$	110.7	110.6	110.4
Ni $3p$	66.2	66.2	66.0
Cr $2p_{3/2}$	574.3	574.3	574.3
Cr $3s$	74.3	74.4	74.4
Cr $3p$	41.8	41.7	42.1
B $1s$	188.0	188.0	187.5[a]

[a]The value reported by Hendrickson *et al.* (Ref. 31).

TABLE II. Comparison of the asymmetry index in Ni $2p_{3/2}$ and Cr $2p_{3/2}$ in elemental form with that in a-$Ni_{81}Cr_{15}B_4$ and c-$Ni_{81}Cr_{15}B_4$. The satellite intensities associated with the Ni $2p_{3/2}$ peak for polycrystalline nickel, a-$Ni_{81}Cr_{15}B_4$ and c-$Ni_{81}Cr_{15}B_4$ are compared. Satellite intensity as percentage of total intensity of the main line plus satellite.

Core level	Material	Asymmetry index	Satellite intensity
Ni $2p_{3/2}$	Polycrystalline nickel	1.1	27%
	a-$Ni_{81}Cr_{15}B_4$	1.0	20%
	c-$Ni_{81}Cr_{15}B_4$	1.1	18%
Cr $2p_{3/2}$	Polycrystalline chromium	1.24	
	a-$Ni_{81}Cr_{15}B_4$	1.43	
	c-$Ni_{81}Cr_{15}B_4$	1.39	

on a Philips PW 1729 model using Cu $K\alpha$ radiation. The sample was rinsed in isopropanol and mounted on a molybdenum sample holder with a built-in heater in such a way that the shiny side of the sample could be analyzed. The sample was then introduced into a VG Scientific Ltd. ESCALAB MK II spectrometer for photoelectron spectroscopic analysis. All measurements were performed in a vacuum better than 5×10^{-10} Torr. Mg $K\alpha$ (1253.6 eV) radiation was used for x-ray-photoelectron spectroscopy measurements and He I (21.2 eV) as well as He II (40.8 eV) resonance lines were employed for ultraviolet-photoelectron spectroscopy work. The $Ni_{81}Cr_{15}B_4$ metallic glass sample showed the presence of carbon and oxygen in the XPS survey scan. The sample was thoroughly cleaned, made free of these contaminants by argon-ion bombardment. The argon-ion gun was operated for this purpose at 4 kV and 10 μA for 30 min.

After XPS and UPS analysis of α-$Ni_{81}Cr_{15}B_4$ metallic glass at room temperature, it was sputter cleaned and annealed in an ultrahigh vacuum (UHV) for 2 h at 800 K. After cooling the sample, it was further sputter cleaned before carrying out the XPS and the UPS analysis. The annealed sample was later subjected to XRD analysis which confirmed that the $Ni_{81}Cr_{15}B_4$ sample had crystallized.

XPS and UPS spectra of high-purity nickel and chromium (supplied by Goodfellow Metals, U.K.) were also recorded for comparison with nickel and chromium in the $Ni_{81}Cr_{15}B_4$ sample under identical conditions. Samples were mechanically polished and rinsed with isopropanol before introducing them for analysis. The sputter cleaning was carried out to remove surface contaminants. The Au $4f_{7/2}$ line located at a binding-energy value of 84.0±0.1 eV was used as a standard in this work.

III. RESULTS

The x-ray-photoelectron spectra and ultraviolet-photoelectron spectra presented here are normalized to the same height after linear background subtraction. In Fig. 1 XPS valence-band spectra for Ni, Cr, a-$Ni_{81}Cr_{15}B_4$ and c-$Ni_{81}Cr_{15}B_4$ are presented and Figs. 2 and 3 give the corresponding spectra obtained with He I (21.2 eV) and He II (40.8 eV) radiation, respectively.

The binding-energy values obtained for various core levels of Ni, Cr, and B in pure elements as well as in a-$Ni_{81}Cr_{15}B_4$ and c-$Ni_{81}Cr_{15}B_4$ are presented in Table I. Except for boron, the observed shifts in the binding energies for both the amorphous and crystalline metallic glasses are very small. However, the general trend appears to be an increase in the binding-energy value for nickel and boron in the metallic glass sample accompanied by either the decrease or negligible change in the binding-energy value for chromium. It is interesting to note that even though the shift in the core level binding energies is relatively small, the changes in the satellite intensity for Ni $2p_{3/2}$ and asymmetry index for Cr $2p_{3/2}$ are significant. These results are summarized in Table II. The satellite peak was observed for Ni $2p_{3/2}$ in pure element and a- and c-$Ni_{81}Cr_{15}B_4$ (Fig. 4) but no satellite for Cr $2p_{3/2}$ is observed.

The variations in DOS for the valence band when going from the crystalline to the amorphous state for metallic glasses are reflected in the ratio of intensity at E_F (I_{E_F}) to the intensity at maximum ($I_{\max}$) for normalized curves. We have presented in Table III these ratios, i.e., $I_{E_F}/I_{\max}$ along with the difference in binding-energy value at $I_{\max}$ and E_F.

TABLE III. The d-band maximum positions in nickel, chromium, a-$Ni_{81}Cr_{15}B_4$, and c- $Ni_{81}Cr_{15}B_4$ are compared. The ratio of intensity at Fermi level (I_{E_F}) and at maximum ($I_{\max}$) indicates the change in the density of states near the Fermi level.

Sample	Energy difference between binding-energy values at $I_{\max}$ and E_F in eV	$I_{E_F}/I_{\max}$
Polycrystalline Ni	0.4	0.89
Polycrystalline Cr	1.5	0.54
a-$Ni_{81}Cr_{15}B_4$	0.5	0.75
c-$Ni_{81}Cr_{15}B_4$	0.5	0.92

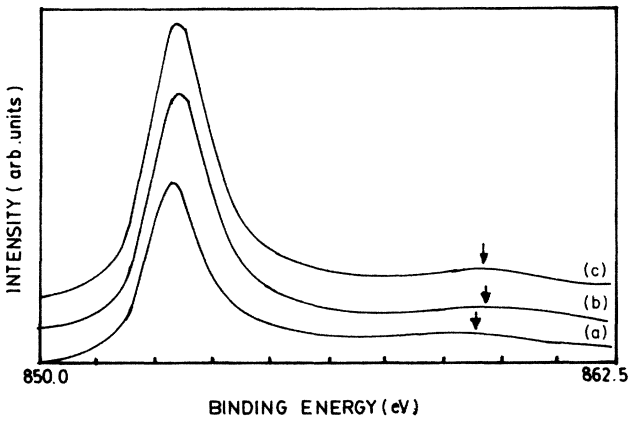

FIG. 4. Ni $2p_{3/2}$ core line for (a) polycrystalline nickel, (b) a-$Ni_{81}Cr_{15}B_4$, and (c) c-$Ni_{81}Cr_{15}B_4$. The satellite line is shown by an arrow.

IV. DISCUSSION

Metallic glasses, which are alloys in the continuous ranges of concentration and the concentrations at which no crystalline phase exists, offer an opportunity to study the correlation between parameters which define the glassy state and the electron properties. Photoemission experiments, where one can vary the excitation energies, yield useful information about the electronic structure, whereas the band-structure calculations, in general, make an important contribution to the understanding of experimental data. Therefore, before discussing our results on a- and c-$Ni_{81}Cr_{15}B_4$ alloys, we briefly discuss the validity of our experimental data on polycrystalline nickel and chromium upon comparison with the available results of theoretical band-structure calculations.[15–19] This forms a base for further understanding of a- and c-$Ni_{81}Cr_{15}B_4$ alloys. Our experimental valence-band curve for nickel [Fig. 1(a)] matches qualitatively well with the theoretical curve.[15–19] The observed d-band width is slightly narrower than that predicted by the theory. The nickel d-band maximum is located at 0.4 eV below the Fermi level and a broad satellite at ~ 6 eV on the high binding-energy side is observed [Fig. 1(a)]; such a satellite, as shown by Fuggle *et al.*[12] and Hillebrecht *et al.*,[20] is associated not only with the valence band but also with each core level. However, the appearance of the satellite very much depends on the number of effective d electrons and its position is controlled by the final state after photoionization. The nickel d band contains 9.4 electrons[21,22] and the d character is reflected in the unoccupied s,p states and vice versa. The ground state for nickel is therefore considered to be a linear combination of d^9 and d^{10} wave functions with appropriate hybridization of s,p states. The total wave function is nearly degenerate in the ground state but when a hole is created either in the valence band or a core level (for example due to photoionization) the degeneracy is lifted and an additional peak (satellite) at about 6 eV appears. Thus, if any change occurs in the number of d electrons because of alloying or compound formation, it would be reflected in the satellite intensity. We shall see later that this forms an important clue while interpreting XPS valence-band data on a- and c- $Ni_{81}Cr_{15}B_4$.

For chromium also [Fig. 1(b)] the agreement between the experimental XPS valence-band curve and theoretical DOS is good. The main peak in both the cases matches and three peaks at about 2.6, 3.3, and 4.1 eV below E_F in the theoretical DOS curve[23] are also reflected in the experimental curve. The d-band peak is observed at 1.5 eV below the Fermi level and the observed d-band width, i.e., 4.8 eV, is large compared with the calculated d-band width (3.8 eV); Asano and Yamashita[24] have reported the calculated d-band width of 4.2 eV. One more aspect of the XPS valence band for chromium is the absence of a satellite hump. The satellite for Cr $2p_{3/2}$ is also not seen in polycrystalline chromium (Fig. 1). The chromium valence band has appropriate mixing of d and s,p character with predominantly d character at the top of the band.[23] As mentioned earlier, it is the effect of the core hole on the ground-state configuration of the element under investigation that gives rise to a satellite at the high binding-energy side with respect to E_F. Moreover, Penn[25] and Tersoff *et al.*[26] have shown that the scattering of the valence electrons from the potential of a valence band or core hole and the availability of many appropriate final states above E_F, into which electrons can scatter, control the intensity of the satellite lines. Furthermore, contribution of empty s,p bands to the satellite is weak because the scattering of d electrons in s,p states has low probability.[20] In chromium there are few DOS at E_F. In addition, the band-structural calculations indicate the presence of an s,p character band just above E_F. The satellite intensity, which is determined by the weight of unoccupied $3d$ character and by its position above E_F (a very much smaller contribution is expected from $3d$ character above E_F, in chromium), is therefore so reduced for chromium that it is not seen in both the valence-band and core level ($2p_{3/2}$) spectra.

In the light of the above discussion we shall now consider carefully the valence-band spectra for a- and c-$Ni_{81}Cr_{15}B_4$ which are shown in Fig. 1. In the $Ni_{81}Cr_{15}B_4$ metallic glass under investigation the number of nickel atoms is large as compared to chromium and boron atoms. It is for this reason that the valence band of a-$Ni_{81}Cr_{15}B_4$ [Fig. 1(c)] appears to be governed mostly by nickel atoms. However, there is also an effect of chromium as depicted by the shift of the peak for a-$Ni_{81}Cr_{15}B_4$ towards the peak of polycrystalline chromium. It also appears that the satellite peak at ~ 6 eV seen in the nickel spectrum disappears in the a-$Ni_{81}Cr_{15}B_4$ curve, and this must be because of total reorganization of the valence band in a-$Ni_{81}Cr_{15}B_4$ because of the joint effect of nickel and chromium. The valence band should also have a contribution from boron. In fact, it has been shown that the boron states lie at about 5 eV below the Fermi level. However, in an x-ray-induced valence band boron states do not appear because of the fact that the photoemission cross section of the boron $2p$ level is smaller than the nickel and chromium core levels.[27] In the light of this, it

is interesting to note that the satellite associated with Ni $2p_{3/2}$ in a-$Ni_{81}Cr_{15}B_4$ shows reduction in intensity (Table II, Fig. 4). The appearance of a weaker satellite means a reduction of the Ni DOS at E_F. The variation of such DOS is also expected to be reflected in the intensity ratio I_{E_F}/I_{max}. Indeed, this ratio in comparison to nickel (which really dominates the valence-band DOS at E_F in the $Ni_{81}Cr_{15}B_4$ metallic glass) is reduced in a-$Ni_{81}Cr_{15}B_4$ (Table III). If one compares this ratio for a-$Ni_{81}Cr_{15}B_4$ with that for Cr one can immediately visualize that the DOS at E_F must also be having overlap from Cr. We shall see later that, indeed, such is the case.

Another probe for the DOS at E_F is the study of the shape of the core line. In general, the shape of the core line is asymmetric because of the excitations of electron-hole pairs at the Fermi edge.[28–30] The presence of more occupied and unoccupied states close to the Fermi level facilitates the creation of electron-hole pairs. The asymmetry, therefore, contains information about the DOS close to E_F which could be correlated to the valence-band spectra. The Ni $2p_{3/2}$ asymmetry index is found to reduce (Table II) in a-$Ni_{81}Cr_{15}B_4$, which further supports the reduction of nickel DOS at E_F. The increase of the asymmetry index for Cr $2p_{3/2}$ in the alloy also shows that the chromium DOS must be overlapping with nickel at E_F. It is also known that the variation of the asymmetry index directly reflects the changes in charge (local density of electrons in an atom) around an atom. The reduction of the asymmetry index for Ni $2p_{3/2}$ and its increase for Cr $2p_{3/2}$ indicates the decrease of charge around the nickel atom and increase of charge around the chromium atom. Such changes in charge on atomic site are expected to affect the binding energies of various levels. Due to the screening effect the outer levels would be affected more as compared to the core levels. It can be seen that the binding energy of Ni $3p$ shifts towards high energy in a-$Ni_{81}Cr_{15}B_4$ with reference to pure elements, whereas in Cr $3p$ such a shift is towards the low binding-energy side. This indicates that there is a transfer of electrons (charge) from nickel to chromium. Such a transfer of electrons would affect the band character of chromium. The s,p band which is just above E_F in chromium would now get filled there by shifting the E_F. This, as mentioned earlier, would influence the $3d$ character which in effect controls the intensity of a satellite. In the case of boron the shift in binding energy for $1s$ (Table I) is found to be towards the high binding-energy side with reference to pure boron binding energy. It is difficult to draw any conclusion from this result. The binding energy for $1s$ given in Table I is as reported by Hendrickson *et al.*[31] It may, however, be pointed out that there are evidences for charge transfer from metalloid to metal[32–34] as well as from met-

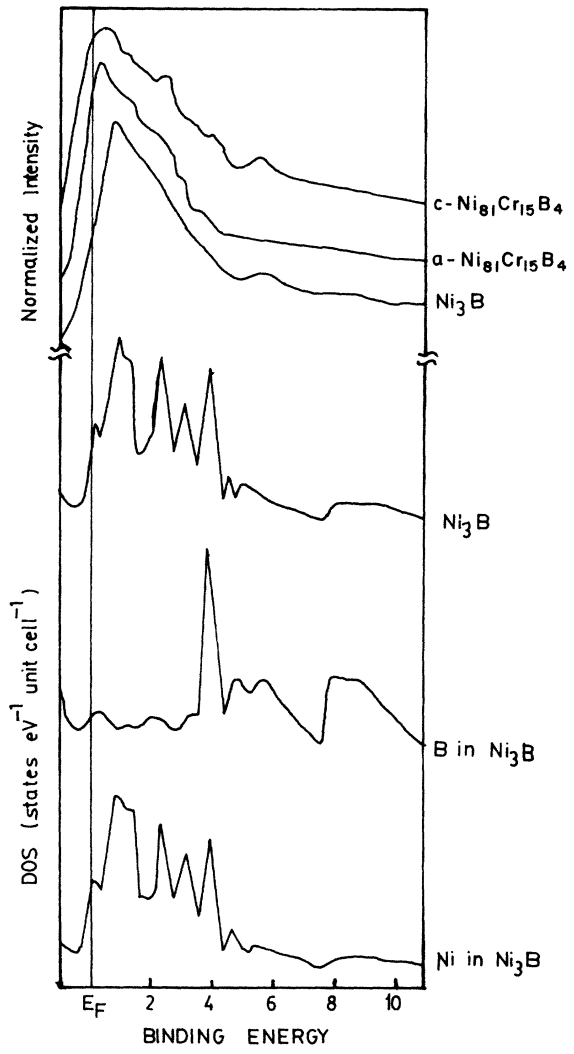

FIG. 5. Theoretical total and site decomposed DOS for Ni_3B (Ref. 39). The experimental valence-band spectra for a-$Ni_{81}Cr_{15}B_4$ along with experimental valence-band spectra for Ni_3B (Ref. 40) are also shown in the figure.

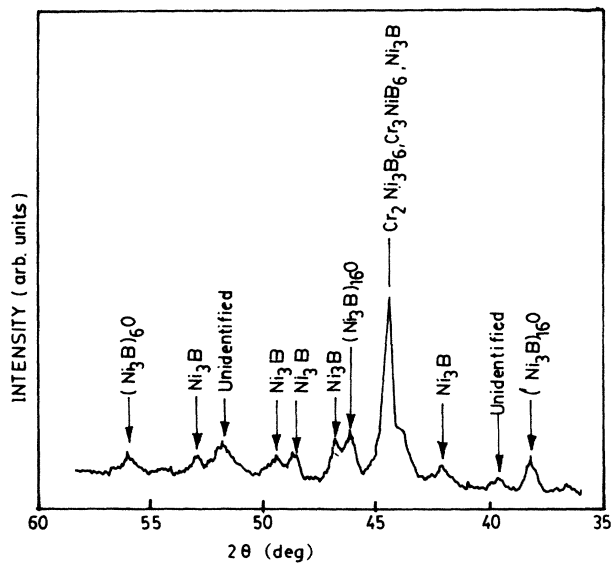

FIG. 6. X-ray diffraction intensity curve for crystallized $Ni_{81}Cr_{15}B_4$ sample.

TABLE IV. Positions of structures (*A*,*B*, . . . in Fig. 2) observed in valence-band spectra from He I source. Ratio I_{E_F}/I_{max} taken similar to that in Table III. Peak of maximum intensity is labeled as (*M*) in the parentheses.

	A	*B*	*C*	*D*	I_{E_F}/I_{max}
Polycrystalline Ni	0.3(*M*)	1.1	4.7	6.7	0.49
Polycrystalline Cr	0.3	0.8(*M*)	2.7	4.8	0.31
a-$Ni_{81}Cr_{15}B_4$	0.69(*M*)	4.2	6.6		0.34
c-$Ni_{81}Cr_{15}B_4$	0.7(*M*)	4.2	6.04		0.35

al to metalloid.[31,35,36]

We shall now discuss the results on *c*-$Ni_{81}Cr_{15}B_4$, which was formed from *a*-$Ni_{81}Cr_{15}B_4$ by crystallizing it under UHV conditions. It can be seen from Fig. 1 that the overall XPS valence-band spectrum for *c*-$Ni_{81}Cr_{15}B_4$ appears to be the same as that of *a*-$Ni_{81}Cr_{15}B_4$ with similar width (5.5 eV for *a*-$Ni_{81}Cr_{15}B_4$ and 5.7 eV for *c*-$Ni_{81}Cr_{15}B_4$). The structures at 2.5 and 4.0 eV appear somewhat more pronounced and an intense peak appears at 5.5 eV. The variation in Ni $2p_{3/2}$ satellite peak intensity, I_{E_F}/I_{max} ratio, and Ni $2p_{3/2}$ asymmetry index are on the same lines (i.e., reduction in the values with reference to pure nickel) as that of *a*-$Ni_{81}Cr_{15}B_4$. This means that in *c*-$Ni_{81}Cr_{15}B_4$ also there is a reduction of DOS at E_F. The Cr $2p_{3/2}$ asymmetry index has comparable values (Table II) to that of *a*-$Ni_{81}Cr_{15}B_4$. This means that even in *c*-$Ni_{81}Cr_{15}B_4$ there is an overlap of Cr levels at E_F. The most interesting observation in XPS valence-band spectra of *c*-$Ni_{81}Cr_{15}B_4$ is the appearance of an additional peak at 5.5 eV (such a peak is not observed in the valence-band spectrum of *a*-$Ni_{81}Cr_{15}B_4$). One would be tempted to attribute it to the satellite [as observed in polycrystalline nickel, Fig. 1(a)] of nickel which may segregate on the surface of the crystallized sample. However, this is not the case, as is shown below.

The band-structure calculations for structurally disordered alloys are complex and therefore theoretical results for ordered alloys are generally compared with experimental data on the valence band. The justification for such a comparison comes from extended x-ray absorption fine-structure (EXAFS),[37] diffraction,[38] nuclear magnetic resonance (NMR) measurements,[39] which have shown that a structural and chemical short-range order comparable to crystalline phases is present in the glassy phase. Hence, band-structure calculations for the ordered alloys with appropriate structure provide a good approximation to the electronic structure of the glassy alloys. Therefore it would be useful to compare calculated DOS for Ni_3B[14] (close-packed Cu_3Au-like structure) with *a*-$Ni_{81}Cr_{15}B_4$ and *c*-$Ni_{81}Cr_{15}B_4$. The comparison with the total and site decomposed calculated DOS for Ni_3B is made with that of experimental results in Fig. 5. In the same figure we have also reproduced the XPS valence-band spectrum for Ni_3B obtained by Amamou *et al.*[40] The shapes of the XPS valence-band spectra for *a*- and *c*-$Ni_{81}Cr_{15}B_4$ are more or less similar to that of the calculated total DOS for the Ni_3B compound. In fact, the structure observed in *c*-$Ni_{81}Cr_{15}B_4$ tallies very well with the structure seen in the total DOS curve for Ni_3B. The peak at 5.5 eV in *c*-$Ni_{81}Cr_{15}B_4$ (which is also seen in the experimental data of Amamou *et al.* on Ni_3B) could be attributed to boron DOS, as seen from comparison with the site decomposed DOS curve for boron. The question could be raised as to why this peak is seen in *c*-$Ni_{81}Cr_{15}B_4$ and not in *a*-$Ni_{81}Cr_{15}B_4$ particularly, when a photoionization cross section at 1253.6 eV Mg $K\alpha$ for boron is known to be smaller when compared to nickel and chromium. This means in *c*-$Ni_{81}Cr_{15}B_4$ an ordered alloy of the Ni_3B type must have been formed and the DOS for such an ordered alloy is reflected in the experimental curve for *c*-$Ni_{81}Cr_{15}B_4$. We have therefore checked the structure of the *c*-$Ni_{81}Cr_{15}B_4$ alloy by XRD. Indeed, the XRD pattern (see Fig. 6) showed the diffraction lines corresponding to the Ni_3B alloy, thereby confirming that that ordered alloy is formed after annealing of *a*-$Ni_{81}Cr_{15}B_4$

It would be interesting to look at the ultraviolet-photoelectron spectra in light of the above results. We have carried out experiments with He I (21.2 eV) and He II (40.8 eV) radiation. At these energies no core levels are ionized. The information about the valence band

TABLE V. Positions of structure (*A*,*B*,. . . in Fig. 3) observed in valence-band spectra from He II source. Ratio I_{E_F}/I_{max} has similar meaning as that given in caption of Table III. Peak of maximum intensity is labeled as (*M*) in the parentheses.

Sample	*A*	*B*	*C*	*D*	*E*	I_{E_F}/I_{max}
Polycrystalline Ni	0.2(*M*)	6.1				0.40
Polycrystalline Cr	0.2	1.0(*M*)	1.7	2.7	3.7	0.31
a-$Ni_{81}Cr_{15}B_4$	0.65(*M*)	7.0				0.35
c-$Ni_{81}Cr_{15}B_4$	0.5(*M*)	2.0	5.6			0.36

with better energy resolution than XPS is obtained, as can be seen from spectra shown in Figs. 2 and 3. The difference between ionization cross sections at low and high energies also contributes to the variation of spectra. The various features observed in He I and He II excited valence-band spectra are summarized in Tables IV and V. It can be seen from Figs. 2 and 3 that overall shapes in the vicinity of the Fermi level and also away from it are strikingly different in *a*- and *c*-$Ni_{81}Cr_{15}B_4$ as compared to polycrystalline nickel and chromium. The fine features observed in the range of 3 eV below E_F for both the nickel and chromium disappear in *a*-$Ni_{81}Cr_{15}B_4$ giving rise to a broad peak with a maximum located between that of nickel and chromium. This is in agreement with our observations of the XPS valence band that the *d* band in *a*-$Ni_{81}Cr_{15}B_4$ is a combination of nickel and chromium *d* states. From Tables IV and V it can be seen by comparing the I_{E_F}/I_{max} ratio for nickel *a*- and *c*-$Ni_{81}Cr_{15}B_4$ that there is a reduction in DOS at E_F, whereas comparison of a similar ratio for chromium indicates, as suggested in the interpretation of the XPS valence band, that chromium *d* states must be overlapping at E_F in the valence band. Two broad weak bands at 4.2 and 6.6 eV below the Fermi level are observed for *a*-$Ni_{81}Cr_{15}B_4$ (Fig. 2). These may be due to the hybridization of metal *d* and metalloid *p* states as well as the metal-metalloid *s* state, respectively. Such hybridized states have been reported for other metal-metalloid glasses. The process of crystallization would trigger clustering of Ni_3B/Cr_3B (it is indeed Ni_3B as seen from XRD, Fig. 6), which would enhance the overlapping of metal-metalloid states. This is reflected in a high density of low-lying states (see the curve for *c*-$Ni_{81}Cr_{15}B_4$) in both Figs. 2 and 3. The pronounced hump at 2 eV in the crystallized sample (Fig. 3) is due to clustering of nickel and boron atoms to form Ni_3B. In general, UPS data is in good agreement with XPS observations.

V. CONCLUSIONS

In this paper we have investigated amorphous and crystalline $Ni_{81}Cr_{15}B_4$ metallic glass samples in order to understand their electronic structure. The results obtained from photoemission experiments ($h\nu = 1253.6$ and 21.2 eV as well as 40.8 eV) for valence-band and core levels have effectively been integrated to arrive at a comprehensive picture of the electronic structures for this alloy. Our investigation suggests the following.

1. The valence band for both *a*- and *c*- $Ni_{81}Cr_{15}B_4$ is made up of nickel 3*d*, chromium 3*d*, and boron 2*p* levels. The hybridized metal-metalloid states account for the high density of low-lying states.

2. At a local level for both *a*- and *c*-$Ni_{81}Cr_{15}B_4$ there is a reduction in DOS at E_F.

3. Crystallization process triggers the formation of clusters of Ni_3B.

4. There is a charge transfer from nickel to chromium.

Our results, where XPS and UPS data have been effectively utilized to arrive at a comprehensive electronic structure, suggest that similar investigations on metal-metal and metal-metalloid glass alloys, as well as their crystalline forms, with controlled variation of constituent elements would lead to better understanding of the interrelationship between composition, structure, stability, and density of states in the valence band.

ACKNOWLEDGMENTS

Two of us (S.K.K. and M.G.T.) thank the Department of Science and Technology (DST) of India for their financial support. This work was supported by DST India.

[1]V. L. Moruzzi, P. Oelhafen, and A. R. Williams, Phys. Rev. B **27**, 7194 (1983).

[2]J. Kanski and G. Pet'O, Solid State Commun. **51**, 747 (1984).

[3]E. Majkova, P. Duhaj, and P. Mikusik, J. Magn. Magn. Mater. **41**, 155 (1984).

[4]P. Marko, M. Konc, L. Potocky, P. Mitusik, and E. Kisdi-Koszo, J. Magn. Magn. Mater. **41**, 135 (1984).

[5]E. Cartier, Y. Baer, M. Liard, and H.-J. Güntherodt, J. Phys. F **10**, L21 (1980).

[6]A. R. Yavari, J. Phys. F **16**, 687 (1986).

[7]H. S. Chen and K. A. Jackson, in *Treatise on Materials Science and Technology,* edited by Herbert Herman (Academic, New York, 1981), Vol. 20, p. 215.

[8]S. R. Nagel and J. Tauc, Phys. Rev. Lett. **35**, 380 (1975).

[9]P. Haüssler, F. Baumann, J. Krieg, G. Indlekofer, P. Oelhafen, and H.-J. Güntherodt, Phys. Rev. Lett. **51**, 714 (1983).

[10]V. L. Moruzzi, P. Oelhafen, A. R. Williams, R. Lapka, H.-J. Güntherodt, and J. Kubler, Phys. Rev. B **27**, 2049 (1983).

[11]M. G. Thube, S. K. Kulkarni, D. Hüerta, and Arun S. Nigavekar, Phys. Rev. B **34**, 6874 (1986).

[12]John C. Fuggle, F. Ulrich Hillebrecht, R. Zeller, Zygmunt Zolnierek, Peter A. Bennett, and Ch. Freiburg, Phys. Rev. B **27**, 2145 (1983).

[13]L. Ley, O. B. Dabbousi, S. P. Kowalezyk, F. R. McFeely, and D. A. Shirley, Phys. Rev. B **16**, 5372 (1977).

[14]P. Oelhafen, in *Electron Spectroscopy of Metallic Glasses in Glassy Metals II,* Vol. 53 of *Topics in Applied Physics,* edited by H. Beck and H. J. Güntherodt (Springer-Verlag, Berlin, 1983), p. 283.

[15]C. S. Wang and J. Callaway, Phys. Rev. B **15**, 298 (1977).

[16]L. Hodges, H. Ehrenreich, and N. D. Lang, Phys. Rev. **152**, 505 (1966).

[17]J. W. D. Connolly, Phys. Rev. **159**, 415 (1967).

[18]E. I. Zornberg, Phys. Rev. **131**, 244 (1970).

[19]U. Von Barth and L. Hedin, J. Phys. C **5**, 1629 (1972).

[20]F. U. Hillebrecht, J. C. Fuggle, P. A. Bennett, Z. Zolnierek, and C. Freiburg, Phys. Rev. B **27**, 2179 (1983).

[21]N. F. Mott, Adv. Phys. **13**, 325 (1964).

[22]H. Danan, A. Herr, and A. J. P. Meyer, J. Appl. Phys. **39**, 669 (1968).

[23]M. Yasni, E. Hayashi, and M. Shimizu, J. Phys. Soc. Jpn. **29**, 1446 (1970).

[24]S. Asano and J. Yamashita, J. Phys. Soc. Jpn. **23**, 714 (1967).

[25]D. R. Penn, Phys. Rev. Lett. **42**, 921 (1979).

[26]J. Tersoff, L. M. Falicov, and D. R. Penn, Solid State Commun. **32**, 1045 (1979).
[27]W. J. Carter, G. K. Schweitzer, and T. A. Carlson, J. Electron Spectrosc. Relat. Phenom. **5**, 827 (1974).
[28]G. D. Mahan, Phys. Rev. **163**, 612 (1967).
[29]P. Nozières and C. T. de Dominicis, Phys. Rev. **178**, 1097 (1969).
[30]S. Doniach and M. Sunjic, J. Phys. C **3**, 285 (1970).
[31]D. N. Hendrickson, J. M. Hollander, and W. L. Jolly, Inorg. Chem. **9**, 612 (1970).
[32]N. Lundquist, H. P. Myers, and R. Westin, Philos. Mag. **7**, 187 (1962).
[33]R. C. O'Handly and D. S. Boudreaux, Phys. Status Solidi A **45**, 607 (1978).
[34]R. Hasegawa, W. A. Hires, L. E. Kabacoff, and P. Duwez, Solid State Commun. **20**, 1035 (1976).
[35]K. Asami, H. M. Kimura, K. Hashimoto, T. Masumoto, A. Yokoyama, H. Komiyama, and H. Inove, J. Non-Cryst. Solids **64**, 149 (1985).
[36]Nianyi Chen, Pingyi Feng, and Jie Sun, in *Rapidly Quenched Metals,* edited by S. Steeb and H. Warlimont (Elsevier, Amsterdam, 1985), p. 999.
[37]D. Raoux, J. F. Sadoc, P. Lagarde, A. Sadoc, and A. Fontaine, J. Phys. (Paris) Colloq. **41**, C8-207 (1980).
[38]P. Chieux and H. Ruppersberg, J. Phys. (Paris) Colloq. **41**, C-145 (1980).
[39]P. Panissod, D. Aliaga Guerra, A. Amamou, and J. Durrand, Phys. Rev. Lett. **44**, 1465 (1980).
[40]A. Amamou, D. Aliaga Guerra, P. Panissod, G. Krill, and R. Kuntzler, J. Phys. (Paris) Colloq. **41**, C8-396 (1980).